Vol. 2-No.1 (2025) pp. 131-136

### **Research Article**

# Synergistic Evaluation of Ionizing Radiation Shielding in Novel Lead-Free Alloys Using Geant4 MC toolkit

#### Morad Kh. Hamad\*

Al Hussein Technical University, Department of Basic Sciences, Amman-Jordan \* Corresponding Author Email: <a href="mailto:morad.hamad@htu.edu.jo">morad.hamad@htu.edu.jo</a> - ORCID: 0000-0002-5007-7850

## **Article History:**

**DOI:** 10.22399/ijasrar.47 **Received:** Sep. 03, 2025 **Revised:** Nov. 05, 2025 **Accepted:** Nov. 12, 2025

### **Keywords:**

Alloys, Geant4 MC toolkit, Simulation, Phy-X, Photon shielding Abstract: In this study, three lead-free alloys, CrSbSe3, HfSnS3, and ZrSnS3 were selected to investigate their photon shielding properties using Geant4 MC toolkit. The simulated mass attenuation coefficient (MAC) are then benchmarked with theoretical data obtained from Phy-X software demonstrating excellent agreement between the data set with percentage difference below 2% confirming the consistancy between Geant4 MC toolkit and theoretical data. From the simulated MAC, different key shielding parameters such as linear attenuation coefficient (LAC), half-value layer (HVL), mean-free path (MFP), transmission factor, and radiation protection efficiency (RPE) were derived and analyzed in the incident photon energy ranging from 15 keV up to 15 MeV. The findings indicates that all investigated lead-free alloys exhibited superior performance and are highly promising alternative to lead-based shielding materials, particularly in medical and industrial applications.

### 1. Introduction

Radiation shielding materials are important in different technologies such as medical imagining and nuclear power plants [1, 2]. Lead (Pb) has been the traditional shielding material, for decades, because of its desirable properties such as high density and strong photon attenuation capability. However, it is toxic and has a risky impact on the environment [3]. As a result, scientists decide to look for safe, more sustainable materials that can offer similar or even better protections [4-8].

Recently, researchers have turned their attention to lead-free alloys that contain element with moderate to high atomic numbers [9-12]. These materials can effectively attenuate or scatter ionizing radiation while remaining stable and easy to synthesize in simple labs. Among them, CrSbSe3, HfSnS3, and ZrSnS3 are promising candidates. Their mixed compositions combine heavy elements like Antimony (Sb), Hafnium (Hf), and Zirconium (Zr) which enhance photon absorption with lighter chalcogens like Sulphur (S) and Selenium (Se) that enhance structural and chemical stability.

To assess these alloys performance in photon attenuation, Monte Carlo simulation provides a powerful and reliable way to model radiation interactions without the need for extensive experimental setup. The Geant4 MC toolkit is widely used in nuclear and medical physics and allows detailed tracking of photons behaviour through matters [13, 14]. It estimates accurately different key shielding parameters such as the mass attenuation coefficient (MAC), half-value layer (HVL), and mean-free path (MFP).

In this work, we use Geant4 MC toolkit (version 11.2.1) to investigate the photon shielding properties of three selected lead-free alloys, namely, CrSbSe3, HfSnS3, and ZrSnS3. The simulated MAC are then benchmarked with theoretical data obtained from Phy-X software [15]. From Mac, different key parameters such as linear attenuation properties (LAC), HVL, MFP, transmission factor (Trans. Factor), and radiation protection efficiency (RPE) have been calculated and studied. The aim of this study is to identify the most efficient and environmentally friendly options for lead-free radiation shielding.

## 2. Materials and Methods

Three lead-free alloys of CrSbSe3, HfSnS3, and ZrSnS3 were selected to investigate their photon shielding properties. The samples were prepared elsewhere using the convensional solid state reaction [16]. These samples have many needed properties such as chmically stable, non-toxicity, and easy to

prepare in the labe. Besides, CrSbSe3, HfSnS3, and ZrSnS3 samples have relatively high densities, according to the materials project database and shown in Table 1, of 5.65 g/cm<sup>3</sup>, 5.31 g/cm<sup>3</sup>, and 4.08 g/cm<sup>3</sup> respectively [17].

**Table 1.** The investigated lead-free alloys in this study along with their respective densities.

Sample	Element (Weight Fraction %)			Density (g/cm <sup>3</sup> )	Reference
CrSbSe3	(Cr) 0.1266	(Sb) 0.2965	(Se) 0.5769	5.65	[18]
HfSnS3	(Hf) 0.4537	(Sn) 0.3018	(S) 0.2445	5.31	[19]
ZrSnS3	(Zr) 0.2980	(Sn) 0.3878	(S) 0.3142	4.08	[20]

Geant4 is a Monte Carlo simulation toolkit composed of C++ code, designed to simulate particles interactions with matters [13, 14]. It was used to simulate MAC for all samples based on the well-known Beer-Lambert law [21-26]. Comprehesive details on the simulated experimental setup using Geant4 MC toolkit used in this study are prepsented elsewhere [4, 9, 27]. From the simulated MAC, different substantial properties such as LAC, HVL, MFP, Transmission factor, and RPE were calculated and studied.

# 3. Results and Analysis

The Geant4 MC toolkit (v.11.2.1) was utilized to determine the MAC of the selected lead-free alloys in the energy range of 15 keV to 15 MeV. The results were then visually benchmarked with the MAC obtained from Phy-X software, as shown in Figure 1. As can be seen from the figure, both datasets are in excellent agreement, indicating the reliability of using the Geant4 code and providing confidence in the validity of the results. From the simulated MAC, several important shielding parameters were calculated and studied.

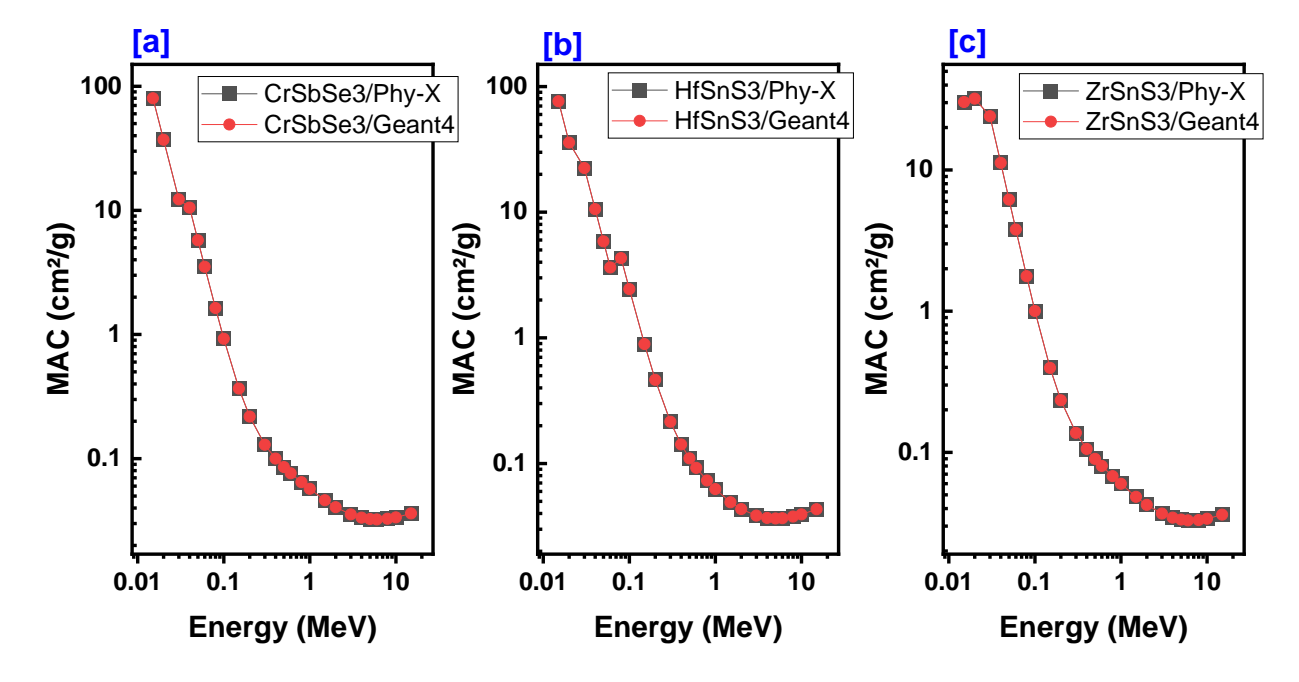


Figure 1. Variation of the mass attenuation coefficient for all lead-free alloys studied in this work with photon energy. Geant4 data is shown in red circles while the Phy-X data is shown in in black squares.

Figure 2 shows the variation of the linear attenuation coefficient (LAC) derived from the MAC for all investigated samples in this study with the incident photon energy. This parameter is important to measure how effectively the selected samples reduce the intensity of incident photons as they pass through them. LAC is simply obtained by multiplying the MAC by the density of each sample. According to

Figure 2, the LAC decreases rapidly as photon energy increases, a typical behaviour of photon interaction with matter. For instance, the LAC at 15 keV is 452 cm<sup>-1</sup>, 406 cm<sup>-1</sup>, and 124 cm<sup>-1</sup> for CrSbSe3, HfSnS3, and ZrSnS3, respectively. As energy increases to reach 0.1 MeV, the LAC declines to 5.22 cm<sup>-1</sup>, 12.95 cm<sup>-1</sup>, and 4.09 cm<sup>-1</sup> for the same samples, respectively. The main reason for this drop in this energy range can be attributed to the photoelectric effect, which predominates in this region. The observed spikes in the LAC are ascribed to the presence of the K-edge of the X-ray from the heavy elements used in preparing these compositions. As energy increases to reach 1 MeV, the LAC decreases gradually due to the dominance of Compton scattering. At very high energy, above 1 MeV, pair production starts to contribute, and the differences in LAC values between all samples become less pronounced.

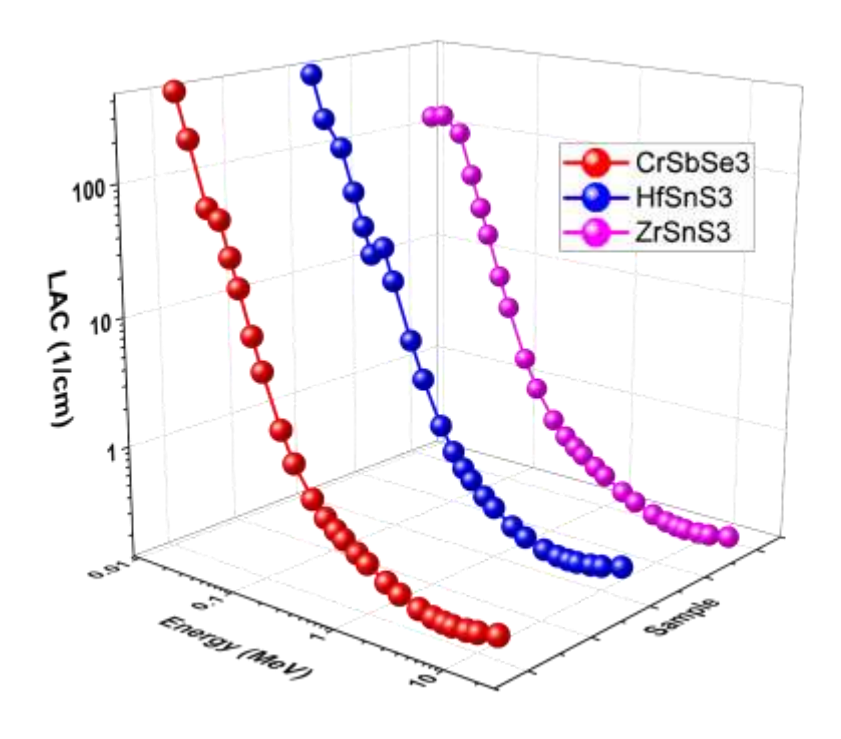
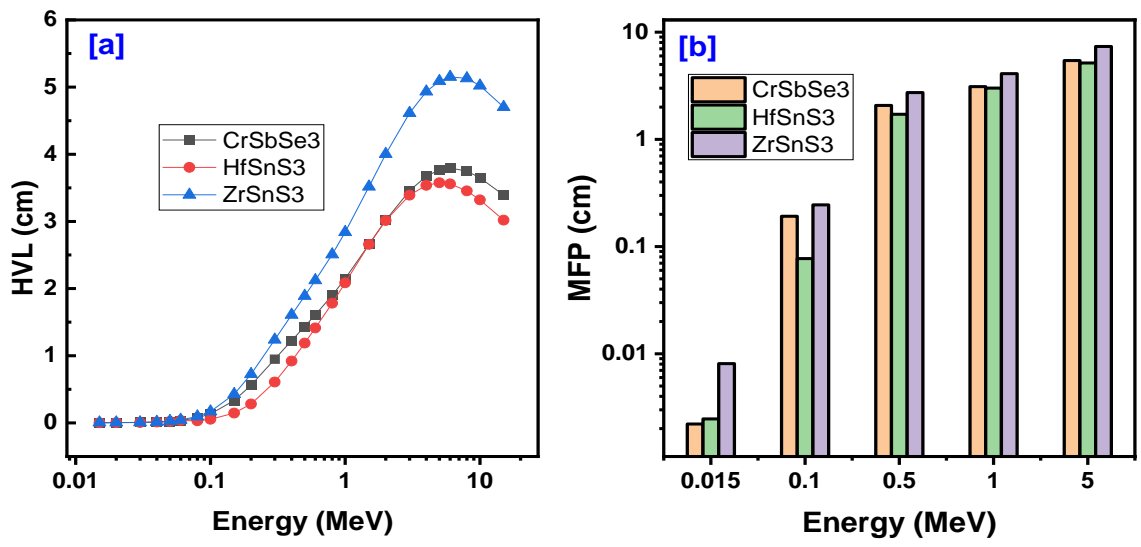


Figure 2. The linear attenuation coefficient for all lead-free alloys studied in this work versus incident photon energy in log-log scale.

Different shielding parameters were derived from the LAC. For instance, Figure 3(a) shows the variation of the half-value layer (HVL) with incident photon energy for all investigated lead-free alloys in this study. This important parameter indicates the thickness of the alloys needed to reduce the incident photon intensity to half (i.e., 50%). It is worth noting that HVL is inversely related to the LAC, indicating that the sample with the higher LAC exhibits a lower HVL and vice versa. As can be seen from the figure, HVL increases with photon energy, indicating a decrease in shielding efficiency as the photoelectric effect decreases and Compton scattering starts to dominate, especially in the intermediate energy region up to 1 MeV. For example, at 0.05 MeV, the photoelectric effect is the main interaction mechanism, and the HVL is as low as 0.02 cm to 0.03 cm for all investigated alloys in this study. As energy increases to reach 1 MeV, where Compton scattering is the dominant interaction mechanism, HVL increases to 2 cm to 3 cm in all samples. In the high-energy region, at 5 MeV, for example, HVL reaches 5 cm in the ZrSnS3 sample, indicating that pair production is emerging in this region.

Figure 3(b), on the other hand, shows the mean free path (MFP) for the studied samples at different selected energies covering the main three interaction mechanisms. MFP is another important concept in ionizing radiation shielding that gives the average distance a photon travels in the studied alloys before undergoing an interaction. It can be directly derived from the LAC by calculating its inverse. Clearly, MFP is inversely proportional to LAC and increases with photon energy. At 15 keV, the MFP is 0.00221 cm, 0.00247 cm, and 0.00809 cm for CrSbSe3, HfSnS3, and ZrSnS3, respectively, where the photoelectric effect dominates. As energy increases to 0.5 MeV, Compton scattering starts contributing, and

the MFP records 2.07227 cm, 1.7145 cm, and 2.72788 cm for CrSbSe3, HfSnS3, and ZrSnS3, respectively. When energy increases to 5 MeV, pair production may contribute, and the MFP is 5.43527 cm, 5.15749 cm, and 7.34197 cm for CrSbSe3, HfSnS3, and ZrSnS3, respectively.



**Figure 3.** (a) The half-value layer (HVL) for all lead-free alloys studied in this work versus incident photon energy in log-log scale. (b) the mean-free path (MFP) for all studied samples at different selected photon energy covering all interaction mechanisms.

Figure 4 shows both (a) the transmission factor and (b) radiation protection efficiency (RPE) for a 1 cm sample of CrSbSe3, HfSnS3, and ZrSnS3 alloys. In the low-energy region, just below 0.1 MeV, it is observed that the transmission factor is approximately 0% for all samples, which means that a 1 cm sample of all alloys investigated in this work can effectively block photons up to 0.1 MeV. This result is further confirmed in the RPE results, where it reaches 100% for all samples studied up to 0.1 MeV. The elevated RPE at lower energy levels is mainly attributed to the photoelectric effect, which facilitates substantial photon absorption. As energy increases to reach 0.5 MeV, for instance, Compton scattering becomes the dominant interaction mechanism, and the transmission factor starts increasing to reach ~62%, 56%, and 69% for CrSbSe3, HfSnS3, and ZrSnS3, while the RPE at 0.5 MeV decreases to reach ~38%, 44%, and 31% for CrSbSe3, HfSnS3, and ZrSnS3, respectively. In the high-energy region, such as 5 MeV, pair production becomes increasingly relevant at even higher energy levels, further reducing the RPE and increasing the transmission factor. The transmission factor at this energy increases to ~83%, 82%, and 87%, and the RPE decreases to ~17%, 18%, and 13% for CrSbSe3, HfSnS3, and ZrSnS3, respectively.

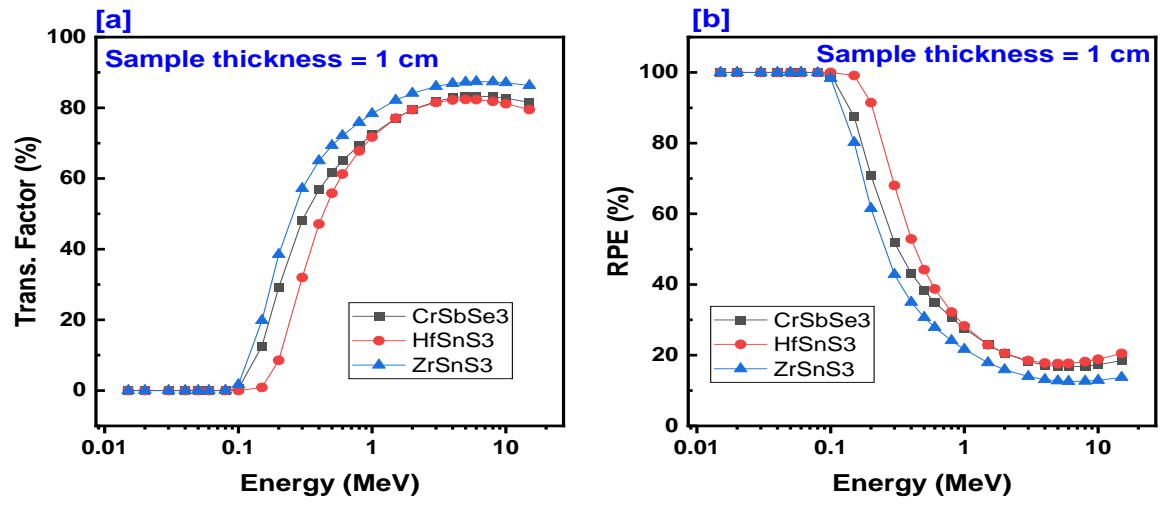


**Figure 4.** (a) The transmission factor and (b) radiation protection efficiency for a 1 cm thickness of each leadfree alloys investigated in this study versus incident photon energy.

### 4. Conclusion

In this study, we investigated the photon attenuation properties of three selected lead-free alloys, namely CrSbSe3, HfSnS3, and ZrSnS3 using Geant4 MC toolkit. The results are then benchmarked against Phy-X software. The two datasets demonstrate excellent agreement, confirming the reliability of the computational approach in getting the mass attenuation coefficient (MAC). Different shielding parameters were derived from the MAC such as LAC, HVL, MFP, transmission factor and RPE. Analysis of these parameters revealed clear energy dependent shielding behaviour. Among the investigated alloys, differences in compositions significantly affect shielding performance at different photon energies, highlighting the potential of those lead-free materials as effective, environmentally friendly alternatives for ionizing radiation shielding applications.

#### **Author Statements:**

- Ethical approval: The conducted research is not related to either human or animal use.
- **Conflict of interest:** The authors declare that they have no known competing financial interests or personal relationships that could have appeared to influence the work reported in this paper
- **Acknowledgement:** The authors declare that they have nobody or no-company to acknowledge.
- **Author contributions:** The authors declare that they have equal right on this paper.
- **Funding information:** The authors declare that there is no funding to be acknowledged.
- **Data availability statement:** The data that support the findings of this study are available on request from the corresponding author. The data are not publicly available due to privacy or ethical restrictions.

### References

- [1] Parker, H. M. O., & Joyce, M. J. (2015). The use of ionising radiation to image nuclear fuel: A review. Progress in Nuclear Energy, 85, 297-318. https://doi.org/10.1016/j.pnucene.2015.06.006
- [2] Jefferson, S., Roberts, R., Ley, F., & Rogers, F. (1968). INDUSTRIAL APPLICATIONS OF IONIZING RADIATIONS. In Elsevier eBooks (pp. 335–383). <a href="https://doi.org/10.1016/b978-1-4831-9958-0.50013-4">https://doi.org/10.1016/b978-1-4831-9958-0.50013-4</a>
- [3] Collin, S., Baskar, A., Geevarghese, D. M., Ali, M. N. V. S., Bahubali, P., Choudhary, R., Lvov, V., Tovar, G. I., Senatov, F., Koppala, S., & Swamiappan, S. (2022). Bioaccumulation of lead (Pb) and its effects in plants: A review. Journal of Hazardous Materials Letters, 3, 100064. https://doi.org/10.1016/j.hazl.2022.100064
- [4] Hamad, M. K. (2026). Optical, photon interaction, and radiation shielding performance of Ho2O3-doped borate glasses modified with ZnO and CaO. Materials Research Bulletin, 194, 113785. <a href="https://doi.org/10.1016/j.materresbull.2025.113785">https://doi.org/10.1016/j.materresbull.2025.113785</a>
- [5] Hamad, M. K. (2025). Enhancing ionizing radiation shielding properties with PbO and ZnO substitutions in B2O3–BaO–TiO2 novel glass system. Radiation Physics and Chemistry, 229, 112499. https://doi.org/10.1016/j.radphyschem.2024.112499
- [6] Hamad, M. K. (2025). Effect of WO3 on structural, optical, mechanical, and ionizing radiation shielding properties of borate-tellurite glass network. Ceramics International, 51(8), 9763-9771. <a href="https://doi.org/10.1016/j.ceramint.2024.12.407">https://doi.org/10.1016/j.ceramint.2024.12.407</a>
- [7] Alajerami, Y.S.M., Morsy, M.A., Mhareb, M.H.A. et al. Structural, optical, and radiation shielding features for a series of borate glassy system modified by molybdenum oxide. Eur. Phys. J. Plus 136, 583 (2021). https://doi.org/10.1140/epjp/s13360-021-01582-x
- [8] Hamad, R., Hamad, M. K., Mhareb, M., Sayyed, M., Alajerami, Y., Dwaikat, N., Almessiere, M., Imheidat, M. A., & Ziq, K. A. (2022). Structural and radiation shielding features for BaSn1-xZnxO3 perovskite. Physica B: Condensed Matter, 638, 413925. https://doi.org/10.1016/j.physb.2022.413925
- [9] Hamad, M. K. (2025). On the ionizing radiation protection properties of different chromium-based alloys: A study with the Geant4 Monte Carlo toolkit. Annals of Nuclear Energy, 213, 111134. https://doi.org/10.1016/j.anucene.2024.111134
- [10] Farrag, E. A., Hamad, M. K., Ali, A., Abdelmonem, A., & Al-Taani, H. (2024). Unveiling the shielding potential: Exploring photon and neutron attenuation in a novel lead-free XCr2Se4 chalcogenide Spinals alloys

- with MCNP 4C code. Radiation Physics and Chemistry, 226, 112337. https://doi.org/10.1016/j.radphyschem.2024.112337
- [11] Hamad, R.M., Hamad, M.K., Dwaikat, N. et al. Assessment of FexSe0.5Te0.5 alloy properties for ionizing radiation shielding applications: an experimental study. Appl. Phys. A 128, 574 (2022). https://doi.org/10.1007/s00339-022-05721-8
- [12] Hamad, M. K. (2023). Evaluation of photon shielding properties for new refractory tantalum-rich sulfides Ta9(XS3)2 alloys: A study with the MCNP-5. Annals of Nuclear Energy, 184, 109687. https://doi.org/10.1016/j.anucene.2023.109687
- [13] Agostinelli, S., Allison, J., Amako, K., Apostolakis, J., Araujo, H., Arce, P., Asai, M., Axen, D., Banerjee, S., Barrand, G., Behner, F., Bellagamba, L., Boudreau, J., Broglia, L., Brunengo, A., Burkhardt, H., Chauvie, S., Chuma, J., Chytracek, R., . . . Zschiesche, D. (2003). Geant4—A simulation toolkit. Nuclear Instruments and Methods in Physics Research Section A: Accelerators, Spectrometers, Detectors and Associated Equipment, 506(3), 250-303. <a href="https://doi.org/10.1016/S0168-9002(03)01368-8">https://doi.org/10.1016/S0168-9002(03)01368-8</a>
- [14] Allison, J., Amako, K., Apostolakis, J., Arce, P., Asai, M., Aso, T., Bagli, E., Bagulya, A., Banerjee, S., Barrand, G., Beck, B., Bogdanov, A., Brandt, D., Brown, J., Burkhardt, H., Canal, P., Cano-Ott, D., Chauvie, S., Cho, K., Yoshida, H. (2016). Recent developments in Geant4. Nuclear Instruments and Methods in Physics Research Section A: Accelerators, Spectrometers, Detectors and Associated Equipment, 835, 186-225. https://doi.org/10.1016/j.nima.2016.06.125
- [15] Şakar, E., Özpolat, Ö. F., Alım, B., Sayyed, M., & Kurudirek, M. (2019). Phy-X / PSD: Development of a user friendly online software for calculation of parameters relevant to radiation shielding and dosimetry. Radiation Physics and Chemistry, 166, 108496. <a href="https://doi.org/10.1016/j.radphyschem.2019.108496">https://doi.org/10.1016/j.radphyschem.2019.108496</a>
- [16] Lu, Y., Yu, W., Zhang, Y., Zhang, J., Chen, C., Dai, Y., Hou, X., Dong, Z., Yang, L., Fang, L., Huang, L., Lin, S., Wang, J., Wang, J., Li, J., & Zhang, K. (2023). Synthesis and Broadband Photodetection of a P-Type 1D Van der Waals Semiconductor HfSnS3. Small, 19(44), e2303903. https://doi.org/10.1002/smll.202303903
- [17] Jain, A., Ong, S. P., Hautier, G., Chen, W., Richards, W. D., Dacek, S., Cholia, S., Gunter, D., Skinner, D., Ceder, G., & Persson, K. A. (2013). Commentary: The Materials Project: A materials genome approach to accelerating materials innovation. APL Materials, 1(1). <a href="https://doi.org/10.1063/1.4812323">https://doi.org/10.1063/1.4812323</a>
- [18] Data retrieved from the Materials Project for CrSbSe3 (mp-15236) from database version v2025.09.25. <a href="https://doi.org/10.17188/1191071">https://doi.org/10.17188/1191071</a>
- [19] Data retrieved from the Materials Project for HfSnS3 (mp-8725) from database version v2025.09.25. https://doi.org/10.17188/1312614
- [20] Data retrieved from the Materials Project for ZrSnS3 (mp-17324) from database version v2025.09.25. <a href="https://doi.org/10.17188/1192450">https://doi.org/10.17188/1192450</a>
- [21] Al-Sarray, E., Akkurt, İ., Günoğlu, K., Evcın, A., & Bezır, N. (2017). Radiation shielding properties of some composite panel. Acta Physica Polonica A, 132(3), 490–492. <a href="https://doi.org/10.12693/aphyspola.132.490">https://doi.org/10.12693/aphyspola.132.490</a>
- [22] Davraz, M., Pehlivanoğlu, H., Kilinçarslan, Ş., & Akkurt, İ. (2017). Determination of Radiation Shielding of Concrete Produced from Portland Cement with Boron Additives. Acta Physica Polonica A, 132(3), 702–704. <a href="https://doi.org/10.12693/aphyspola.132.702">https://doi.org/10.12693/aphyspola.132.702</a>
- [23] Özavci, S., & Çetin, B. (2017). Radiation shielding properties of mortars and plasters used in historical buildings. Acta Physica Polonica A, 132(3–II), 986–987. https://doi.org/10.12693/aphyspola.132.986
- [24] Çetin, B., Yalçin, Ş., Aktas, B., & Albaşkara, M. (2017). Investigation of Radiation Shielding Properties of Soda-Lime-Silica Glasses Doped with Different Food Materials. Acta Physica Polonica A, 132(3–II), 988–990. https://doi.org/10.12693/aphyspola.132.988
- [25] Evcin, O., Evcin, A., Bezir, N., Akkurt, İ., Günoğlu, K., & Ersoy, B. (2017). Production of barite and boroncarbide doped radiation shielding polymer composite panels. Acta Physica Polonica A, 132(3–II), 1145–1148. <a href="https://doi.org/10.12693/aphyspola.132.1145">https://doi.org/10.12693/aphyspola.132.1145</a>
- [26] Kilinçarslan, Ş., Üncü, İ., Akkurt, İ., Günoğlu, K., Akarslan, F., & Coşkunsu, S. (2017). Determination of Radiation Shielding Properties of Fabrics using Image Processing Method. Acta Physica Polonica A, 132(3–II), 1171–1172. <a href="https://doi.org/10.12693/aphyspola.132.1171">https://doi.org/10.12693/aphyspola.132.1171</a>
- [27] Yaghi, M. A., Sayyed, M., Mhareb, M., Bennal, A., & Hamad, M. K. (2026). Radiation shielding and mechanical performance of lead-free novel glasses: Insights from Geant4 Monte Carlo simulations. Radiation Physics and Chemistry, 239, 113335. https://doi.org/10.1016/j.radphyschem.2025.113335